

USE OF TiO₂ AS A REINFORCEMENT OF CASSAVA STARCH/PVA COMPOSITES ON MOISTURE-RESISTANT PROPERTIES OF TRIBOELECTRIC NANOGENERATOR (TENG) FILM

ARIS ANSORI^{1,2*}, SUDJITO SOEPARMAN¹, DENNY WIDHIYANURIYAWAN¹
AND TEGUH DWI WIDODO¹

¹*Department of Mechanical Engineering, Universitas Brawijaya
Jl. Mayjen Haryono 167 Malang 65145, East Java, Indonesia*

²*Department of Mechanical Engineering, Universitas Negeri Surabaya,
Campus Ketintang Surabaya 60231, East Java, Indonesia*

*Corresponding author: arisansori@unesa.ac.id

(Received: 30 July 2022; Accepted: 3 February 2023; Published on-line: 4 July 2023)

ABSTRACT: High humidity environments can accelerate the transmission, neutralization, or dissipation of frictional charges on the frictional surface of solid-solid triboelectric nanogenerator films (TENGs), which can reduce the output power. The moisture resistance properties of the TENG triboelectric film are needed to overcome these problems. Therefore, this study discusses the role of the TiO₂ nanofiller in cassava starch (CS) and polyvinyl alcohol (PVA) nanocomposite matrix that can increase triboelectricity through the formation of hydrogen bonds and the provision of oxygen-free electrons. The research method was to incorporate different concentrations of TiO₂ nanoparticles (0%, 0.5%, 1%, 5%, 10% wt, and 15% wt) into the CS-PVA nanocomposite matrix using the solvent casting method. The results showed an increase in surface polarity which was more triboelectric-positive due to the CS-PVA hydroxyl group interacting with water molecules. Increasing the concentration above 5% wt TiO₂ increases the density of the CS-PVA nanocomposite film which can significantly reduce water vapor permeability (WVP) and increase water resistance. The TENG performance of the CS-PVA/TiO₂ nanocomposite film with a concentration of 15% wt TiO₂ under conditions of high humidity (RH, 95%) resulted in an output voltage of 2.5-fold (~70.5 V to ~180 V), and the output current increased 2.6-fold (~5.2 μA to ~13.7 μA).

ABSTRAK: Persekitaran berkelembapan tinggi dapat mempercepat penghantaran, penutralan, atau pelepasan cas geseran pada permukaan geseran filem nanopengeluaran triboelektrik pepejal (TENG), di mana mengurangkan pengeluaran tenaga. Sifat rintangan lembapan filem triboelektrik TENG diperlukan bagi mengatasi masalah ini. Oleh itu, kajian ini membincangkan peranan pengisi nano TiO₂ dalam matriks nanokomposit kanji ubi kayu (CS) dan polivinil alkohol (PVA) yang dapat meningkatkan triboelektrik melalui pembentukan ikatan hidrogen dan bekalan elektron bebas oksigen. Kaedah kajian ini adalah dengan menggabungkan kepekatan nanozarah TiO₂ berbeza (0%, 0.5%, 1%, 5%, 10%, dan 15%) ke dalam matriks nanokomposit CS-PVA menggunakan kaedah tuangan pelarut. Dapatan kajian menunjukkan peningkatan kekutuban permukaan yang lebih positif-triboelektrik adalah disebabkan oleh kumpulan hidroksil CS-PVA yang berinteraksi dengan molekul air. Pertambahan jisim kepekatan TiO₂ melebihi 5% meningkatkan ketumpatan filem nanokomposit CS-PVA yang boleh mengurangkan kebolehtelapan wap air dan meningkatkan rintangan air dengan ketara. Prestasi TENG filem nanokomposit CS-PVA/TiO₂ dengan jisim kepekatan TiO₂ 15% dalam keadaan berkelembapan tinggi (RH, 95%) menghasilkan voltan keluaran sebanyak 2.5 kali ganda

(~70,5 V kepada ~ 180 V), dan arus keluaran meningkat 2.6 kali ganda (~ 5,2 μ A kepada ~ 13,7 μ A).

KEYWORDS: nanocomposite films; TiO_2 ; cassava starch/PVA; moisture resistant; triboelectric nanogenerators (TENG)

1. INTRODUCTION

A triboelectric nanogenerator (TENG) is a micro/nanoscale energy harvesting device that utilizes static electric charges or the triboelectric effect between two materials that have different electronegativities [1]. TENG's working mechanism is a combination of contact electrification and electrostatic induction to convert mechanical energy that is abundant in the environment into electrical energy. The TENG structure consists of two electrodes made of copper or aluminum, where electrode 1 is attached to the tribo-positive layer and electrode 2 is attached to the tribo-negative layer, the TENG structure is presented in Fig. 1a. There are four working modes of TENGs, namely; contact mode, slide mode, single electrode mode, and freestanding mode [2,3]. The working modes of TENGs are presented in Fig. 1.

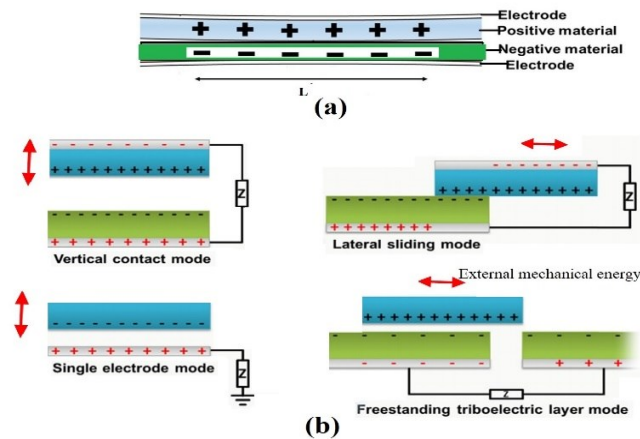


Fig. 1: The working modes of TENG (a) contact electrification phenomena between different triboelectric materials, (b) The four working modes of TENG.

The schematic diagrams of working TENG, are presented in Fig. 2. The working TENG mechanism that converts mechanical energy into electricity consists of four steps. In step I, the two layers of the triboelectric layer (tribo-positive layer and tribo-negative layer) are in contact with one another, where the contact of two surfaces of the triboelectric film layer has not resulted in charge (Fig. 2a). In step II, the application of mechanical energy to the tribo-positive layer 1 causes friction to occur, reduces the contact area between the tribo-positive layer 1 and the tribo-negative layer 2, and causes a charge difference on the surface of the triboelectric film layer. Then, electrons will flow from electrode 1 to electrode 2 through the outer circuit (resistor) to balance the surface charge on the two triboelectric layers until the contact of the two triboelectric layers is free (Fig. 2b). In step III, the sliding of the tribo-positive layer 1 optimally causes the contact of the two triboelectric layers to completely separate and there is a charge balance between the two triboelectric layers, so that there is no flow of electrons between electrode 1 and electrode 2 (Fig. 2c). In step IV, the tribo-positive layer 1 moves and creates friction and surface contact again between the tribo-positive layer 1 and the tribo-negative layer 2 in the opposite contact direction in stage II, this causes electrons to flow through an external circuit (resistor) from electrode 2 to

electrode 1 to balance the surface charges on the two triboelectric layers with opposite directions of electron flow (Fig. 2d) until the two triboelectric layers return to full contact again at the stage I position. The sliding and closing of the triboelectric layers periodically generate an alternating current [4].

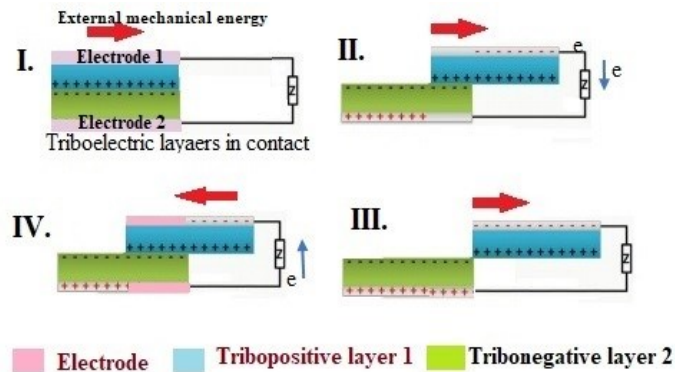


Fig. 2: Schematic diagrams working of TENG.

TENG was first developed by Wang et al. in 2013, The research was carried out utilizing the triboelectric effect of materials to harvest mechanical energy into electricity and showed high energy conversion efficiency. [5]. TENG has become a promising energy conversion device to convert mechanical energy into electrical energy due to the capacity of triboelectric materials. TENG can be a solution for new and sustainable energy harvesting, such as wind [5], ocean waves [6], human movement [7], rotational motion [8-11], flowing water [12], vibration [13], and other energy sources.

In general, the TENG device consists of two friction materials and electrodes at the top and bottom of the device wherein, physical contact between two friction materials with different levels of electronegativity can induce a triboelectric charge which can produce a potential decrease when separated by mechanical forces and increase the flow of electrons between the electrodes via an external circuit. The dominant factor that determines the performance of TENG's output is the TENG friction material, such as the use of nanocomposite friction materials on a nanoscale which has the advantages of mechanical strength, toughness, flexibility, transparency, dielectric, thermal, or electrical conductivity properties which show an effective and efficient TENG performance improvement [6,7].

In the previous research report, the use of nanocomposite films showed an improved TENG performance. One such nanocomposite material is polydimethylsiloxane (PDMS), a silicon-based organic polymer compound (organosilicon). PDMS nanocomposite films with TiO_2 deposition can cause changes in oxygen vacancies on the PDMS surface which can contribute to electron exchange and trapping and have an impact on increasing TENG output power [8]. Poly (vinylidene fluoride) (PVDF) polymer with TiO_2 NPs as filler can improve dielectric properties [9]. Polydimethylsiloxane (PDMS) with different TiO_x weight ratios as a function of dielectric constant control with 5% rutile TiO_x and 7% TiO_x anatase phase produces the highest TENG output of ~ 180 V/ $8.2 \mu\text{A}$ and 211.6 V/ $8.7 \mu\text{A}$ [10]. TiO_2 nanoparticles 0.2% wt in Portland cement increased the mechanical strength 1.3-fold and 3-fold the power density of 265 mW/m^2 than pure Portland cement [11]. However, TENG's output power may decrease due to high humidity environmental conditions. When the humidity is high, the water molecules in the air absorb on the surface of the friction film pair and form a conductive water film, which can increase the frictional interface conductivity and accelerate the frictional charge transfer or neutralize the charge on the next

contact. These conditions, will generate different frictional charges when the TENG solid-solid films rub against each other [12].

Several methods have been reported to solve the problem, such as; creating a hydrophobic or superhydrophobic film to reduce the adsorption of water molecules on the friction surface and loosen the texture of the structure to increase the permeability of the material [13,14]. For example, Shen et al., using a hydrophobic polyvinylidene fluoride (PVDF) film, showed the performance of TENG at 55% relative humidity with an output current of 28 μA , a voltage of 345 V, and a power density of 1.3 W/m^2 [15]. Lv et al. made a TENG single electrode using a hydrophobic ionic liquid that showed high stability performance in various weather conditions (humidity up to 80%) [16]. Zhou et al. used a TENG with superhydrophobic PDMS interlayer film that can maintain electrical output under initial conditions up to relative humidity of 80% [17]. However, modification of the hydrophobic surface when humidity is high cannot completely solve the problem of decreasing the output performance of solid-solid TENG. In addition, the hydrophobic or superhydrophobic film process requires a complicated film-making process, and its manufacture is not easy to apply to some materials.

Currently, the use of biomaterials rich in hydroxyl groups has begun to be developed as a TENG triboelectric film, several studies have shown that TENGs output performance is very good by utilizing the ability to bind water molecules by forming hydrogen bonds. In addition, biomaterials are expected to replace synthetic polymers (PDMS, PVDF, PET, and Teflon) which still dominate the TENG film. Meanwhile, several applications of TENG triboelectric films are made from biomaterials rich in hydroxyl groups, such as; pure potato starch exhibits high output performance of 60 mV to 300 mV per 4 cm^2 area [18]. The triboelectric film of tapioca starch rich in hydroxyl groups can enhance the triboelectricity effect by improving water molecules on the friction film surface through hydrogen bonding [19,20]. Potato starch biomaterials with 0.5% CaCl_2 showed an increase in triboelectric performance; the highest voltage output (1.2 V) was three times higher than that of pure starch [21]. In addition, the use of starch biomaterials has advantages, such as biocompatibility and biodegradability [18,19][21-23], abundant availability, easy processing, bring inexpensive, possessing hydroxyl groups, amorphous crystal structure, and rheological properties that can provide the required resistance for TENG triboelectric film applications [24].

However, starch biomaterials still have problems in the application of TENG triboelectric films, such as poor mechanical properties, ease of dissolving on prolonged contact with water, and poor tribological properties in high humidity environments and low moisture resistance when exposed to high humidity conditions as a friction film. Therefore, to increase the functionality of starch biomaterials is to modify starch biomaterials into nanocomposite films. To the best of our knowledge, the use of TiO_2 nanoparticles as a starch biomaterial nanofiller with moisture resistance characteristics has not been reported. Meanwhile, in this study, a type of nanocomposite film was made using a composite matrix of cassava starch (CS) and PVA with TiO_2 nanofiller to increase moisture resistance. Polyvinyl alcohol (PVA), rich in hydroxyl groups with the addition of TiO_2 , will cause intra/intermolecular interactions between TiO_2 nanoparticles and adjacent OH groups of PVA through hydrogen bonds and form stable complex composites. PVA compatibility increases with the addition of TiO_2 into the film due to the formation of C-O-Ti. Meanwhile, the starch/PVA mixture changed the structure of the starch/PVA composite film by forming C-H bond groups from alkyl groups in both starch and PVA. After incorporating TiO_2 filler into the starch/PVA mixture, C-O bonds will form at the macromolecular level, and intramolecular hydrogen bonds are formed between two neighboring OH groups on the

same side of the plane of the carbon chain. This allows for increased miscibility and compatibility between starch/PVA and TiO_2 with the formation of hydrogen and C-O-Ti bonds which can affect the characteristics of the nanocomposite film [25-27]. Meanwhile, the basis for using TiO_2 nanofillers is that TiO_2 contains oxygen atoms that can be easily dispersed in a polar biopolymer matrix without surface modification. In addition, chemical bonds and electrostatic interactions between oxygen atoms on the metal oxide surface and functional groups in the polymer matrix make the nanoparticles disperse in the polymer matrix [28].

Meanwhile, the special emphasis in this study is to investigate the effect of TiO_2 in the CS-PVA polymer blend on the physicochemical, water resistance, and electrical properties of the nanocomposite films and the TENG characterization of the CS-PVA/ TiO_2 nanocomposite films as positive friction surfaces and thin-film commercial polyimides as negative friction partners. We compared the results and analyzed the effect of TiO_2 on the moisture properties of the CS-PVA nanocomposite films. The results of the measurement of the output voltage and current of TENG CS-PVA nanocomposite film without TiO_2 produced an output voltage and current of ~ 25.5 V and ~ 3.6 μA and with 0.5% wt TiO_2 output voltage of ~ 50 V and an output current of ~ 5.9 μA (relative humidity /RH, 15%). In this case, there was a significant increase in the effect from TiO_2 in the CS-PVA polymer blend. The optimal increase of TENG output voltage and current at a weight ratio of 15% wt TiO_2 at high humidity (RH, 95%) achieved a 2.5-fold increase in output voltage (~ 70.5 V to ~ 180 V), and an output current of 2.6-fold (~ 5.2 μA to ~ 13.7 μA). The addition of a weight ratio above 5% wt TiO_2 can reduce the water vapor permeability by 65%. Therefore, these CS-PVA/ TiO_2 nanocomposite films have the potential for TENG films under high humidity environmental conditions.

2. EXPERIMENTAL METHODS

2.1 Materials

The starch used in the experiment was cassava starch produced by PT. Budi Starch & Sweetener.Tbk. in Indonesia, polyvinyl alcohol (PVA) with an average molecular weight of $M_w = 89,000$ – $98,000$, was procured from Sigma Aldrich. Anatase TiO_2 nanoparticles with a particle size of 20 nm were purchased from Sigma-Aldrich, glycerol (99% purity, clear, colorless, and density: 1.261 g/cm^3), aquades, and other chemicals NaOH, HCl, and NaCl were used to control humidity (RH, 15%, 55%, and 95%) from Sigma-Aldrich and Merck.

2.2 Fabrication of Cassava Starch (CS)-PVA/ TiO_2 Nanocomposite Films

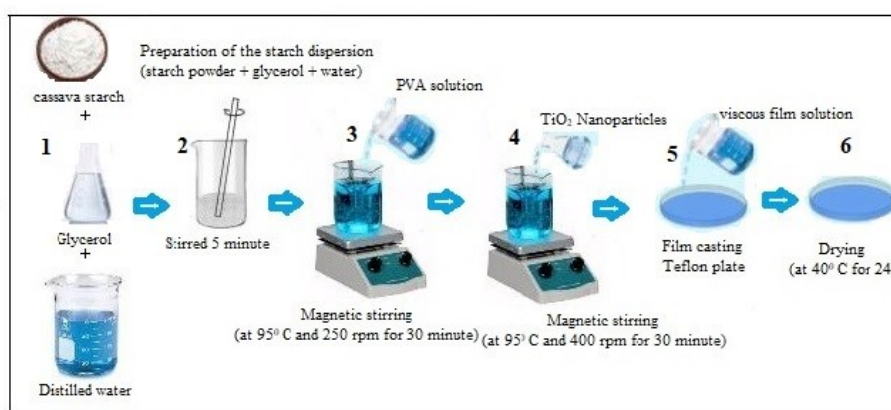


Fig. 3: Preparation of CS/PVA- TiO_2 nanocomposite films by solvent casting method.

Figure 3 describes the making of cassava starch (CS)/PVA nanocomposite films with TiO_2 nanofiller using the solvent casting method. The step of making cassava starch (CS)/PVA- TiO_2 nanocomposite films consists of six steps. In step 1, the constant weight ratio of the CS/PVA mixture (70:30), cassava starch (4.2 g) was determined and dispersed with distilled water (50 mL) in borosilicate glass, and the addition of glycerol (3 g) served as a plasticizer. In step 2, the mixture of CS powder and glycerol was mechanically stirred for 5 minutes until a homogeneous solution was produced. In step 3, the mixture of CS powder and glycerol was stirred with a magnetic stirrer at 250 rpm at a temperature of 95 °C for 30 minutes to obtain a gelatinized starch suspension. Meanwhile, a solution of 1.8 g PVA with 40 mL of distilled water was prepared in the same way in another borosilicate glass, and a clear PVA solution was produced. Mixing of the two solutions (CS solution/PVA solution) was carried out at room temperature with continued stirring with a magnetic stirrer (250 rpm, 95 °C) for 30 minutes. In step 4, the TiO_2 was incorporated into the CS/PVA solution with different polymer weight ratios (0%, 0.5%, 1%, 5%, 10%, and 15% wt), and continuous stirring was carried out using a magnetic stirrer at 400 rpm, and temperature 95 °C for 30 minutes. In step 5, the production of nanocomposite films occurred, where the resulting CS/PVA- TiO_2 viscous solution was poured into Teflon molds (radius 50 mm) with the same volume of solution in each mold to produce relatively the same thickness of film samples; residual air was removed from the solution in a vacuum for 10 minutes using a vacuum machine. In step 6, the drying of the film was carried out in a hot air oven at 40 °C for 24 hours. The dry film was then carefully peeled off from the Teflon mold and produced a film with an average thickness of 100 μm . The resulting nanocomposite films were kept in a zippered bag until tests were carried out to reduce water absorption according to the Ramirez method [29].

2.3 Fabrication of CS-PVA/ TiO_2 Nanocomposite Film-Based TENGs

Figure 4 describes the structure of the TENG mode rotary-disk freestanding (RDF-TENG).

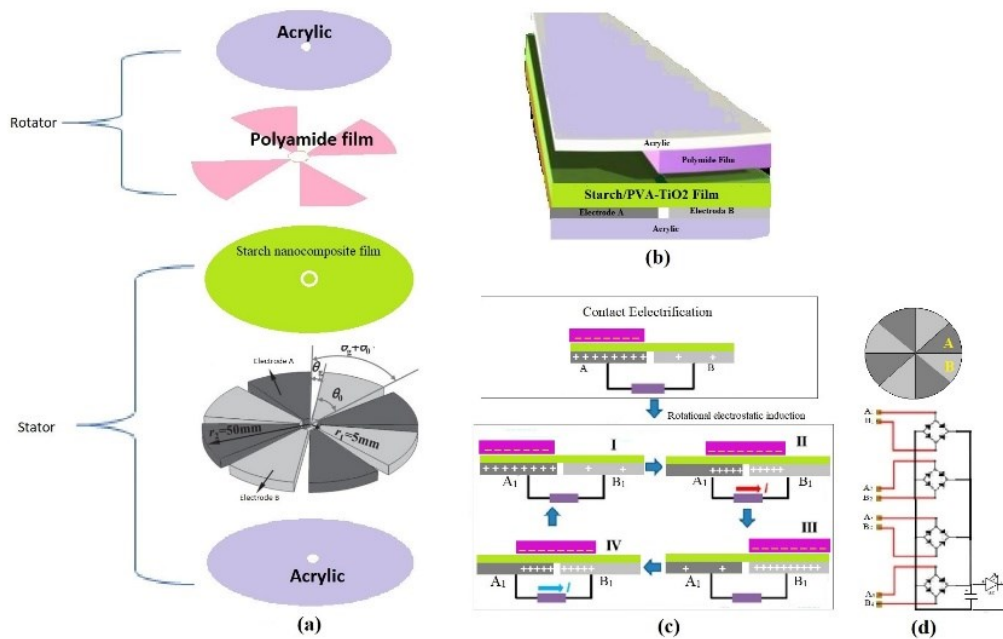


Fig. 4: Schematic of triboelectric nanogenerator based on CS-PVA/ TiO_2 nanocomposite film (a) Structure of rotor and stator (b) TENG component arrangement (c) Freestanding electret rotary (FER) working mechanism (d) TENG electrical circuit.

Rotor structure parameters with the number of film segments (n) = 4, outer radius (r_2) = 50 mm, inner radius (r_1) = 5 mm, were made of commercial polyimide thin film (0.03 mm) as a tribo-negative film glued to an acrylic surface (radius = 50 mm). Meanwhile, the stator structure parameters consisting of CS/PVA-TiO₂ nanocomposite films were cut to form an equal-interval electrode model with the number of film segments (n) = 8, outer radius (r_2) = 50 mm, inner radius (r_1) = 5 mm, and the nanocomposite film thickness was 100 μ m. Next, the cut nanocomposite film was glued to the copper foil (electrode film A and B). Where the tip of the copper foil electrode was slightly exaggerated to connect the external circuit with the help of a conducting wire so that electrons could flow into the external circuit. External mechanical energy used a DC electric motor that was connected to the TENG rotor shaft in a freestanding rotational mode. Meanwhile, the gap between the rotor and stator was controlled with a distance of 0.10 mm to keep the friction between the surface of the polyimide film and the CS/PVA-TiO₂ nanocomposite film stable. The freestanding-electret rotary (FER) TENG mode has four steps. In step I, electrode A is parallel to the polyamide electret film, and there is no electrostatic induction effect of rotating rotor. In step II, the polyamide electret is parallel to the positions of electrodes A and B causing the charge at electrode A to be transferred to electrode B through an external load (resistor) and generating a current and voltage across the load resistor. In step III, the polyamide electret is parallel to electrode B, and in step IV, the polyamide electret will go to electrode segment A and when parallel to electrode A and electrode B will generate current and voltage. A schematic of triboelectric nanogenerator based on CS-PVA/TiO₂ nanocomposite film is presented in Fig. 4.

2.4 Physicochemical Characterizations

2.4.1 Chemical, Crystalline Structure and Morphological Characterization

The functional groups of the nanocomposite films were analyzed using Fourier transform infrared spectroscopy (FTIR) with an IRPrestige-21 spectrophotometer (Shimadzu, USA). FTIR measurements were carried out at room temperature ($25 \pm 1^\circ$ C) in the wave number range of 600–4000 cm^{-1} with a resolution of 2 cm^{-1} and an average of more than 64 scans. The degree of crystallinity of the film samples was recorded using a PANalytical Xpert Pro diffractometer with Cu K α radiation at 40 kV and 40 mA, using a 20 mm Ni filter. All sample films were scanned between $2\theta = 5^\circ$ to 69.99° at $5^\circ/\text{min}$ at a measurement temperature of 25° C. Morphological analysis of nanocomposite film by Scanning Electron Microscope (FESEM) FEI Quanta FEG 650 to explore the effect of TiO₂ filler on the cell structure of the CS-PVA polymer mixture. The dry film sample was sprayed with gold-palladium under vacuum conditions to increase its conductivity. The test was carried out at a voltage of 15xKV with a magnification of 500x.

2.4.2 Water Vapor Permeability (WVP)

The combination of Fick's and Henry's laws for the diffusion of vapors or gases through the film is used as the basis of the method for calculating WVP. The standard ASTM E96 test method (ASTM, 1993) was used to test the WVP of nanocomposite films [41]. In the initial step of the test, the film sample was cut into a circle with a radius of 1.75 cm and tightly mounted on the top surface of a special permeation cup containing CaCl₂ anhydrous. After weighing the initial weight, the cup was stored in a desiccator containing a saturated NaCl solution with a constant relative humidity (RH) of 75% at 25° C. The temperature in the desiccator was maintained at 25° C throughout the experiment. Permeation cup weights were recorded at 24-hour intervals until a constant weight gain was achieved. The amount of water vapor permeating through the film was calculated from the increase in cup weight

and plotted as a function of time. Measurement of WVP ($\text{gm}^{-1}\text{s}^{-1}\text{Pa}^{-1}$) was performed three times using Eq. (1).

$$WVP = \frac{m \cdot d}{A \cdot t \cdot \Delta p} \left(\frac{g}{m \cdot Pa \cdot s} \right) \quad (1)$$

where m = increase in cell mass over a certain period, t = time, d = average film thickness, A = effective film area, and p = difference in water vapor pressure on both sides of the film. The WVP value of the nanocomposite films in this paper represents the effective permeability, which reflects the moisture barrier properties of the films under the humidity and temperature conditions used.

2.4.3 Degradability Tests

The degradability test was carried out to analyze the resistance of the CS-PVA/TiO₂ nanocomposite films in water. In the initial step of testing, the sample nanocomposite film was cut to a size of (2 x 3 cm), then the sample film was immersed in distilled water for a certain time until the sample film was destroyed.

2.5 Electrical Output Measurement

The performance test of the nanocomposite film on the TENG unit was carried out in a closed cylindrical chamber with the same humidity control. The cylinder chamber was equipped with two inlets to circulate dry air and moist air, and one outlet was used to regulate air circulation in the cylinder to achieve the required relative humidity in the room accurately. The external mechanical energy of the rotor used a DC V = 24-volt, 0-500 rpm electric motor. Measurement of output voltage and current used a digital oscilloscope (DSOX6004A Digital Storage Oscilloscope) with a load resistance of 100 M Ω , before the testing film was put in a closed box for 24 hours with adjusted humidity control (15%, 55 %, and 95%) with a saturated salt solution.

3. RESULTS AND DISCUSSION

3.1 Analysis of Chemical, Structural, and Morphological of Nanocomposite Films

Structural analysis can be observed from the FTIR spectrum of the material in the range of 4000-700 cm^{-1} are presented in Fig. 5a, where the molecular bond spectra of the CS-PVA polymer matrix and the change after incorporation of TiO₂ filler can be seen, which has several characteristic peaks reflecting the structure of the two biopolymers. The transmittance band of about 3285 cm^{-1} was determined from the stretching vibration of the hydroxyl group (-OH) in CS and PVA polymers having a hydroxyl-rich average. The peak transmittance band of 1641.42 cm^{-1} indicates the formation of hydrogen bonds in pure starch due to the flexion of the -OH molecule and shows the hygroscopic nature of the starch polymer. Characteristics of the bending of C-OH are in the 1205 cm^{-1} transmittance band. The peak at 770-1120 cm^{-1} is associated with the stretching of the C-O bond of the macromolecular portion, where an intramolecular hydrogen bond is formed between two adjacent OH groups that are on the same side of the plane of the C-C carbon chain of the C-O-C group of the unit glucose in starch [37].

Pure PVA showed hydroxyl and acetate groups, where the intermolecular and intramolecular hydrogen -OH bonds were shown in a wider band at 3296.35 cm^{-1} . The structure of the alkaline group confirmed the peak in the transmission band 1480-1190 cm^{-1} associated with the planar buckling vibrations of C-H and O-H in both CS and PVA. The

presence of a carbonyl group (C=O) is indicated by the 1732 cm^{-1} transmission band and a hydrocarbon (alkane) group in PVA is indicated by a peak at 1373.32 cm^{-1} , as previously reported by Abdullah [30]. Meanwhile, the chemical interaction between CS-PVA polymer molecules that causes changes in the characteristic spectral peaks of the composite, the C–OH hydrocarbon group is estimated to come from the C–O vibrations, which is confirmed by the peak of $1000\text{--}1250\text{ cm}^{-1}$. In addition, the vibration of the –OH group confirmed the absorption peak in the range of $3300\text{--}3000\text{ cm}^{-1}$. The formation of the C–H alkene functional group due to the mixing of starch-PVA which was confirmed at a wavelength of $675\text{--}995\text{ cm}^{-1}$ and C–H alkane which was confirmed at a wavelength of $2850\text{--}2970\text{ cm}^{-1}$.

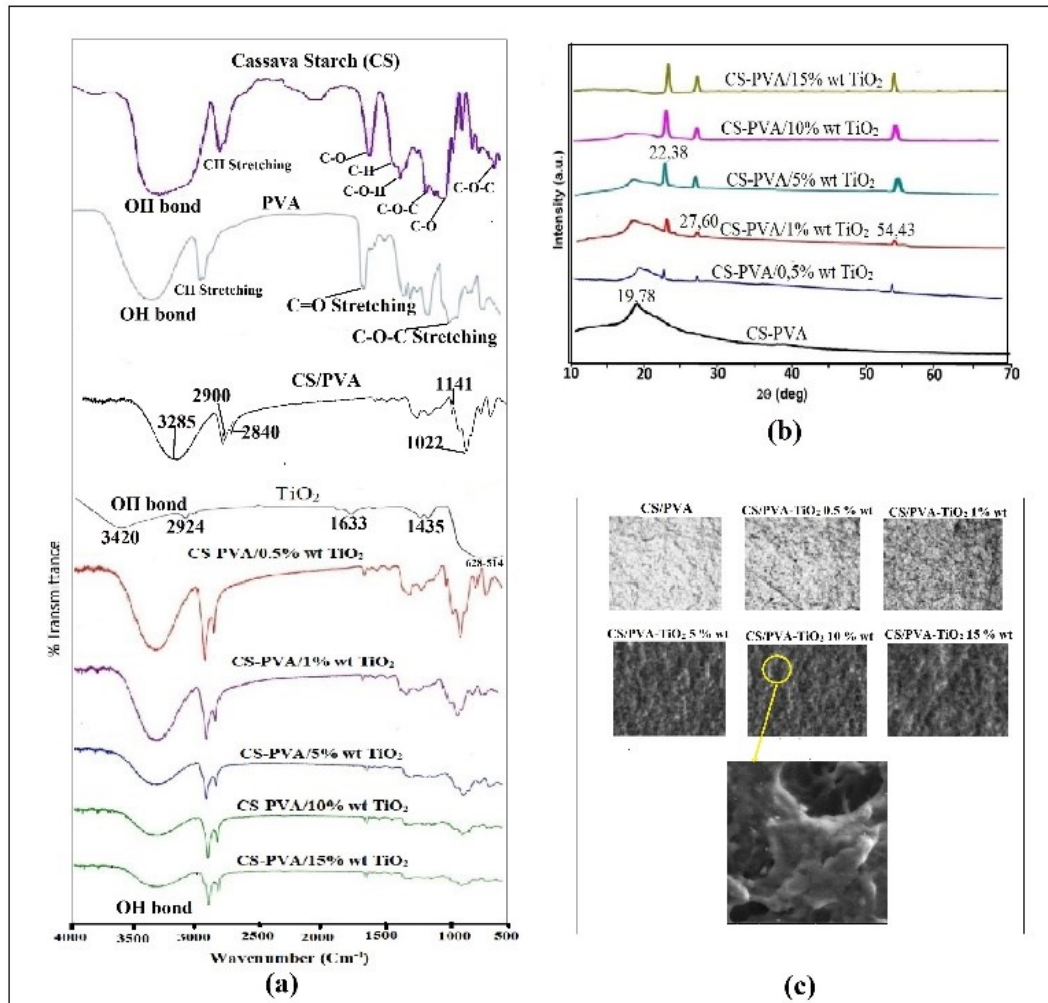


Fig. 5: Physicochemical characterizations of CS-PVA/TiO₂ nanocomposite films.
 (a) FTIR spectra of cassava starch-PVA/TiO₂, (b) XRD pattern of cassava starch film,
 (c) SEM of CS-PVA nanocomposite film.

In addition, the C–H functional group of the aromatic ring was confirmed at the wavelength of $690\text{--}900\text{ cm}^{-1}$. The mixing of CS-PVA polymer showed flexural vibrations of the hydrogen bonding of the –OH group at 1710.86 cm^{-1} and the C–O strain at $1050\text{--}1300\text{ cm}^{-1}$. The stronger interaction of CS-PVA molecules is shown by intermolecular interactions through the formation of hydrogen bonds with water vapor molecules which can increase triboelectricity. At low concentrations (below 15% TiO₂ wt) in the CS-PVA polymer mixture in the FTIR spectrum, the vibration peaks did not show any additional peaks. This may be due to the overlapping bands of the CS-PVA components. However, the

increase in TiO₂ concentration (above 1% TiO₂ wt) showed a slight shift in the peak positions of several bands in the range of 900-1100 cm⁻¹. It is assumed that the absorption band at 1000 cm⁻¹ is associated with the TiO₂ crystal domains hydrated into the CS-PVA polymer matrix. In addition, the titanium ions of the TiO₂ particles can interact with the hydroxyl groups of CS-PVA, which make the nanocomposite films highly compatible.

Figure 5b shows the XRD pattern of the sample film, the cassava starch film produced peaks at $2\theta = 15.73^{\circ}$, 16.51° , 17.23° , 19.69° , 22.14° , and 24.37° whereas, an important diffraction peak was located at 19.69° , which indicates strong intermolecular and intramolecular hydrogen bonds and is indicative of a semi-crystalline structure. This is not much different from the signal of the 20° peaks of cassava starch reported by Bergo et al. [31], and Adamu et al. [32]. Meanwhile, the CS-PVA composite sample formulation produced peaks at $2\theta = 13.11^{\circ}$, 17.21° , 19.76° , and 24.54° , which indicated a change in peak. These peaks can reveal that polymer cassava starch (CS) is dispersed in PVA, which can change the characterization of the films [33,34]. The incorporation of TiO₂ filler into CS-PVA with variations in TiO₂ concentration below 1% wt showed peak changes that were not easily visible at low concentrations. However, increasing the concentration above 1% by weight showed peaks at $2\theta = 22.38^{\circ}$, 27.60° , and 54.43° in semicrystalline structure nanocomposite films and indicated the presence of titanium dioxide embedded in the CS-PVA polymer.

Figure 5c shows the morphology of the polymer mixture of cassava starch (CS)-PVA and the morphological changes of the nanocomposite films after the addition of TiO₂ can be observed from the material micrograph. The ability of starch granules to interact with various ceramic and mineral particles can hold these particles, which causes the added TiO₂ to adhere to the surface of the starch granules well. Meanwhile, mixing CS-PVA suspension with TiO₂ particles, during the gelatinization process, the TiO₂ particles remain attached to the surface of the starch granules and interact with the continuous phase macromolecules of water-soluble amylose and PVA, this process most likely occurs through hydrogen bonding. The SEM photos show morphologically the resulting film has a heterogeneous surface relief. The TiO₂ filler particles were evenly distributed within the polymer matrix. This can be seen from the sample of the film with a low concentration of TiO₂ (0.5% wt), the filler particles are still individual. This is in contrast with the addition of TiO₂ concentration of more than 1% wt indicating the association of filler particles in the composite. In addition, the presence of TiO₂ particles with a high ratio in the film can create a winding path that prolongs the transport of water vapor molecules.

3.2 Water Vapor Permeability (WVP)

Water vapor permeability (WVP) was used as an indicator of the film's ability to absorb water vapor. WVP values of nanocomposite films from the studied samples are presented in Table 1. WVP values of CS-PVA nanocomposite films with TiO₂ are lower than those without TiO₂. The WVP value was inversely correlated with the addition of TiO₂ concentration in the CS-PVA mixture matrix. WVP value of SC-PVA/TiO₂ nanocomposite films decreased with the addition of more than 1% wt TiO₂. This is due to the presence of hydroxyl groups in the CS-PV mixture making the water vapor molecules easy to diffuse. The addition of TiO₂ nanoparticles formed a denser nanocomposite film structure compared to the unfilled film. The presence of TiO₂ in the CS-PVA matrix forms pathways in the polymer that prolong the transport of water vapor molecules. This result is not much different from the results of previous research reports, the effect of TiO₂ nanofiller in polymer films causes a decrease in moisture penetration of corn starch/PVA-TiO₂ films,

[26], Potato starch/lactucin-TiO₂ composite films [35], and Potato Starch/Montmorillonite-TiO₂ composite films [36].

Table 1: Physical properties of CS/PVA-TiO₂ composites

TiO ₂ content % wt	WVP value ($\times 10^{-7}$ g/m h Pa)
0	9.46 ± 0.84
0.5	8.38 ± 0.80
1	7.54 ± 0.78
5	7.39 ± 0.75
10	7.47 ± 0.58
15	7.48 ± 0.55

3.3 Degradability Testing

The degree of damage film caused by water molecules was tested by immersing the nanocomposite film in distilled water (Fig. 6a).

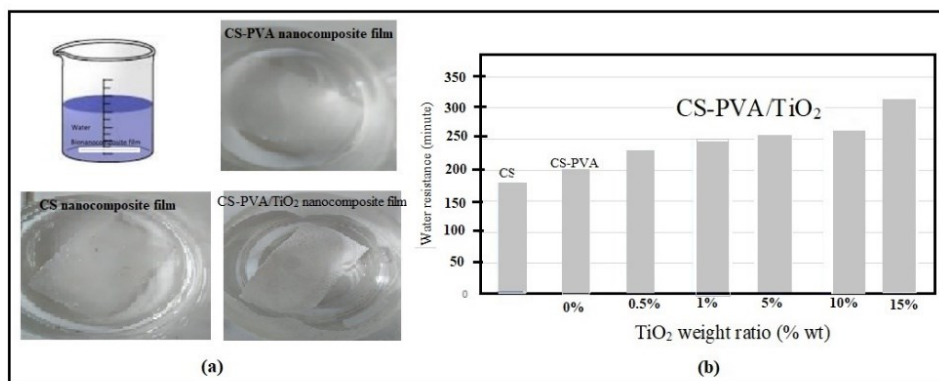


Fig. 6: (a) Test method (b) water-resistance of CS-PVA/TiO₂ nanocomposite films.

The damage rate of CS-PVA nanocomposite films with TiO₂ increased 3-fold compared to without TiO₂. Figure 6b shows the water resistance of CS, CS-PVA, and SC-PVA/TiO₂ films, the resistance of CS films is the lowest compared to CS-PVA and SC-PVA/TiO₂ films. The durability of CS films is affected by the number of hydroxyl groups in the polymer molecules, where the hydroxyl groups bind to water molecules by forming hydrogen bonds. The increase in the number of hydroxyl groups in the CS-PVA film can occur from the intramolecular interaction of the CS-PVA polymer mixture, which can significantly increase the binding of water molecules. The use of reinforcement TiO₂ in the CS-PVA composite increased the durability of the film in water for 315 minutes longer than the CS-PVA film for 200 minutes. The most optimal increase was seen at a concentration of 15% wt TiO₂. The presence of TiO₂ in the CS-PVA polymer mixture made the film denser which increased the absorption capacity of water molecules. In addition, the hydrophobic nature of TiO₂ can also slow down the absorption of water molecules on the film surface.

3.4 Electrical TENG

The schematic diagram of the TENG output test is shown in Fig. 7. Conditioning for humidity levels of 15%, 55%, and 95% were carried out by placing the TENG in a closed cylindrical chamber.

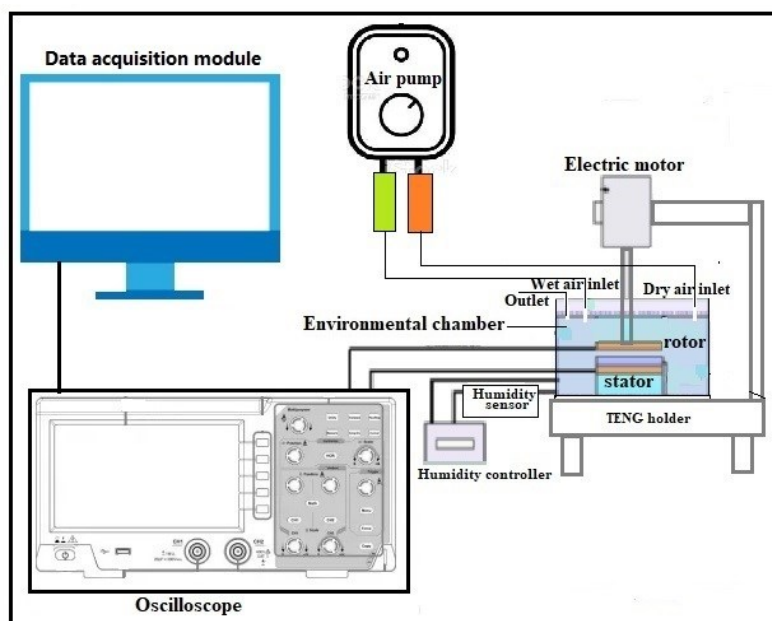


Fig. 7: TENG performance measurements.

The TENG operating mode rotary freestanding (RF-TENG). The stator comprises six sectors of a CS-PVA/TiO₂ nanocomposite film connected to a copper foil electrode, the TENG output circuit uses a rectifier diode to convert AC to DC, and a capacitor as electrical storage before being channeled to the LED load. The rotor rotation speed was controlled stable ($\omega = 200$ rad/s), and the load was 50 M Ω . TENG output performance test with CS-PVA triboelectric film without TiO₂ at a low humidity level (RH, 15%) resulted in an output voltage and current of ~ 25.5 V and ~ 3.6 μ A, while the effect of adding 0.5% wt TiO₂ in the matrix of the CS-PVA nanocomposite showed a 1.9-fold increase in output voltage from ~ 25.5 V to 50 V, and a 1.6-fold increase in output current from ~ 3.6 μ A to ~ 5.9 μ A.

Meanwhile, the addition of TiO₂ in the weight ratio (0% to 15% wt TiO₂) showed a linear increase in voltage and current, respectively, as shown in (Fig. 8b-d). Optimal output voltage and current were achieved at a concentration of 5%wt TiO₂ with a value of 117 V and 10.2 μ A (Fig. 8b). This increase in output voltage and current is due to an increase in the value of the dielectric constant due to the presence of TiO₂ NPs in the CS-PVA polymer mixture which can increase the triboelectric of the film. These results show similarities with some of the results of previous research reports, such as an increase in dielectric properties of poly (vinylidene fluoride) film with TiO₂ NP deposition [9], Dielectric constant changes linearly as a function of weight ratio of PDMS embedded TiO_x NP [10,37], TiO₂ doping on Portland Cement [11], natural rubber (NR)-TiO₂ [38].

In addition, the effect of differences in relative humidity factors (RH, 15%, 55%, and 95%) on the output performance of CS-PVA/TiO₂ film-based TENG at a weight ratio above 5% TiO₂ shows that the resulting voltage and current increase are directly correlated with increased humidity levels (Fig. 8a-c.). The output performance of TENG when the relative humidity condition increased from 15% to 55% (ratio of 15% weight of TiO₂) showed an increase in the output voltage of TENG 1.8 -fold from ~ 70.5 V to ~ 130 V, and the output current increased by 1.1-fold from ~ 5.2 μ A to ~ 5.6 μ A. Enhanced relative humidity of the cylinder chamber is carried out by continuously injecting wet air into the closed cylinder chamber to increase the humidity from 55% to 95% as shown in Fig. 8b-c. Under conditions of relatively high humidity (95%), TENG can produce a 1.4-fold increase in TENG output

voltage from ~ 130 V to ~ 180 V and a 2.4-fold increase in current from ~ 5.6 μA to ~ 13.7 μA . However, the increase in TENG output voltage and current was lower at a TiO_2 weight ratio of less than 5%, about 1.1 times. Meanwhile, the increase in TENG's optimal output voltage and current when humidity is high (RH, 95%) with a concentration of 15% wt TiO_2 can reach 2.5-fold from ~ 70.5 V to ~ 180 V, and the current increases 2.6-fold from ~ 5.2 μA to ~ 13.7 μA .

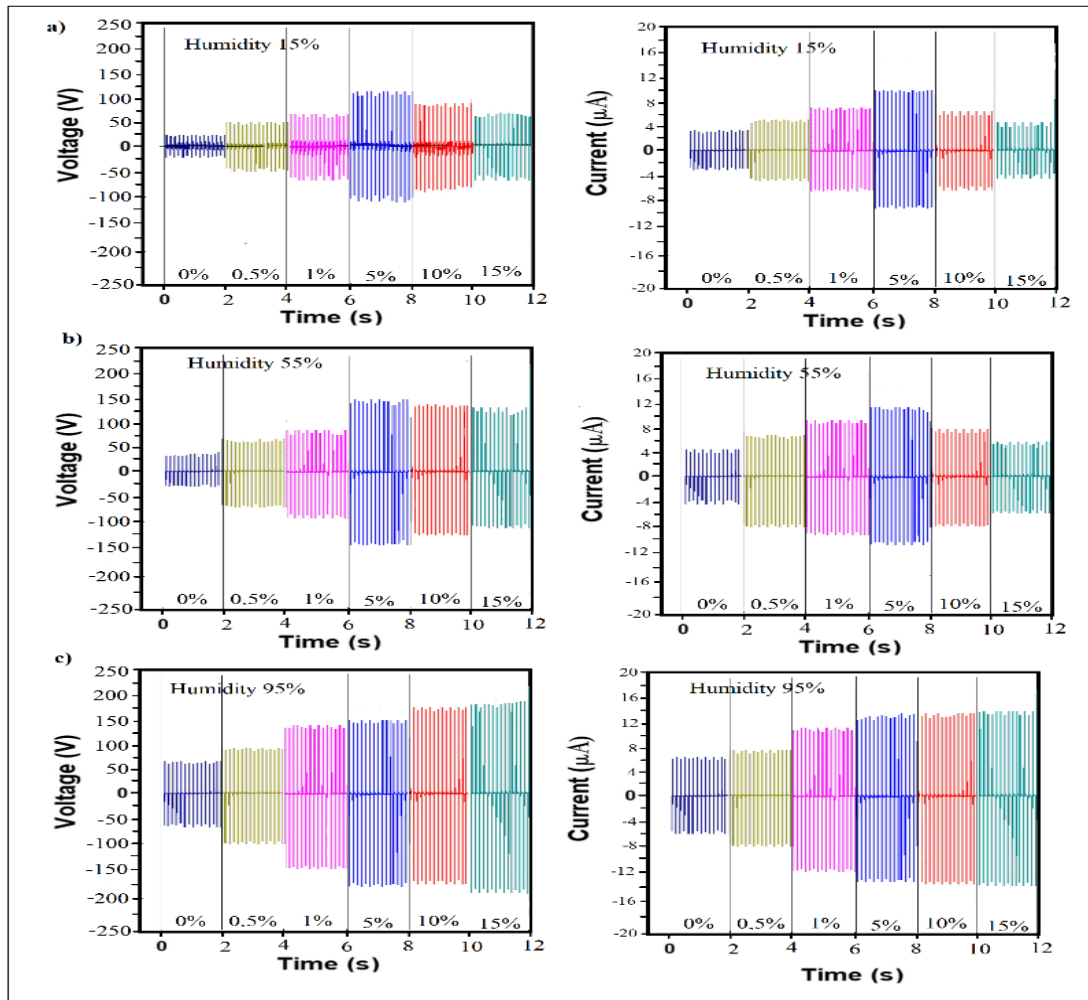


Fig. 8: Output voltage and current at film humidity level:
a) humidity 15%, c) humidity 55%, and c) humidity 95%.

The increase in TENG output voltage and current is caused by the formation of hydrogen bonds between hydroxyl groups and water molecules (when humidity is high) on the surface of the CS-PVA/ TiO_2 nanocomposite film increasing the positive triboelectrification properties of the film. This is not much different from the research reported by Wang et al. using starch polymers rich in hydroxyl groups with the formation of hydrogen bonds with water molecules when humidity is high can increase the output current of TENG based on starch films [39], PVA films rich in hydroxyl chains when humidity is high. High water molecules participate in triboelectric charging [40]. Meanwhile, the effect of the presence of 15% wt TiO_2 concentration in the CS-PVA nanocomposite film showed the most optimal increase at high humidity. The output voltage and current increased with a value to 1.9-fold voltage and 1.8-fold current due to the increase in the density of the nanocomposite film. The density of the film can increase the absorption

of water molecules when humidity is high. In addition, TiO₂ in the CS-PVA matrix can form a winding path that can prolong the transport of water molecules, enhancing the triboelectric properties of the film.

4. CONCLUSIONS

This study presents a method for producing cassava starch (CS)/PVA nanocomposite films using TiO₂ reinforcement. The effects of incorporation of TiO₂ on the structure and properties of the CS/PVA composite were investigated. The FTIR spectra indicate the response of hydroxyl groups in the CS/PVA composite increased after inserting TiO₂ nanoparticles with the formation of hydrogen bonds and C-O-Ti bonds. The interaction between Ti ions and hydroxyl groups forms a complex composite mixture through intra/intermolecular hydrogen bonds. The XRD analysis reveals the TiO₂ concentration (> 1% wt) increased the crystallinity of the nanocomposite film with a semicrystalline structure and variations in crystal shape and uniform crystal size. The SEM photo indicates the TiO₂ can be evenly distributed in the film surface of the CS/PVA composite and resulting in a compatible nanocomposite film. The physical properties of the film increased significantly with the addition of TiO₂ (> 1% wt) with a decreased water vapor permeability (WVP) value $7.39 \pm 0.75 \times 10^{-7}$ g/m h Pa, and the degree of film damage in water decreased by 1.6-fold compared to CS/PVA nanocomposite films without TiO₂ reinforcement. Optimal performance of the CS-PVA/TiO₂ nanocomposite film as a tribo-positive friction film for TENG with a 5% wt TiO₂ concentration, while at high humidity (95% RH) with a 15% wt TiO₂ concentration, the output voltage and current of TENG increased 1.9-fold respectively and the current is 1.8-fold due to the formation of water molecule bonds with the hydroxyl chains, and the availability of free electrons in the film due to the presence of TiO₂ bonds in the CS-PVA matrix. The findings of this study will promote starch-based nanocomposite films that have great potential for tribo-triboelectric nanogenerator (TENG) film applications for high-humidity environmental conditions.

ACKNOWLEDGMENT

This work was supported by the research and community service institute, Universitas Negeri Surabaya (UNESA), under the grant number B/37502/2021.

REFERENCES

- [1] Dzhardimalieva GI, Yadav BC, Lifintseva TV, Uflyand IE. (2021). Polymer chemistry underpinning materials for triboelectric nanogenerators (TENGs): Recent trends. *Eur. Polym. J.*, 142: 110-163. <https://doi.org/10.1016/j.eurpolymj.2020.110163>
- [2] Wang, J., Wu, C., Dai, Y., Zhao, Z., Wang, A., Zhang, T., & Wang, Z. L. (2017). Achieving ultrahigh triboelectric charge density for efficient energy harvesting. *Nature Communications*, 8(1), 1–7. <https://doi.org/10.1038/s41467-017-00131-4>
- [3] Xia K, Fu J, Xu Z. (2020). Multiple-frequency high-output triboelectric nanogenerator based on a water balloon for all-weather water wave energy harvesting. *Adv. Energy Mater.*, 10(28): 1-9. <https://doi.org/10.1002/aenm.202000426>
- [4] Yoon HJ, Ryu H, Kim SW. (2018). Sustainable powering triboelectric nanogenerators: Approaches and the path towards efficient use. *Nano Energy*, 51(June): 270-285. <https://doi.org/10.1016/j.nanoen.2018.06.075>

- [5] Song, G., Kim, Y., Yu, S., Kim, M. O., Park, S. H., Cho, S. M., Velusamy, D. B., Cho, S. H., Kim, K. L., Kim, J., Kim, E., & Park, C. (2015). Molecularly Engineered Surface Triboelectric Nanogenerator by Self-Assembled Monolayers (METS). *Chemistry of Materials*, 27(13), 4749–4755. <https://doi.org/10.1021/acs.chemmater.5b01507>
- [6] Mallakpour S, Jarang N. (2016). Mechanical, thermal and optical properties of nanocomposite films prepared by solution mixing of poly(vinyl alcohol) with titania nanoparticles modified with citric acid and Vitamin C. *J. Plast. Film Sheeting*, 32(3): 293-316. <https://doi.org/10.1177/8756087915597024>
- [7] Khushboo, & Azad, P. (2019). Design and implementation of conductor-to-dielectric lateral sliding TENG mode for low power electronics. In *Advances in Intelligent Systems and Computing* (Vol. 698, Issue May). Springer Singapore. https://doi.org/10.1007/978-981-13-1819-1_17
- [8] Park, H. W., Huynh, N. D., Kim, W., Lee, C., Nam, Y., Lee, S., Chung, K. B., & Choi, D. (2018). Electron blocking layer-based interfacial design for highly-enhanced triboelectric nanogenerators. *Nano Energy*, 50, 9–15. <https://doi.org/10.1016/j.nanoen.2018.05.024>
- [9] Kum-onsa, P., Chanlek, N., Manyam, J., Thongbai, P., Harnchana, V., Phromviyo, N., & Chindaprasirt, P. (2021). Gold-nanoparticle-deposited TiO₂ nanorod/poly(Vinylidene fluoride) composites with enhanced dielectric performance. *Polymers*, 13(13), 1–14. <https://doi.org/10.3390/polym13132064>
- [10] Huynh ND, Park H, Chung K, Choi D. (2018). Effect on TENG performance by phase control of TiO_x nanoparticles. *Compos. Res*, 31(6): 365-370. <http://dx.doi.org/10.7234/composres.2018.31.6.365>
- [11] Sintusiri J, Harnchana V, Amornkitbamrung V, Wongs A, Chindaprasirt P. (2020). Portland Cement-TiO₂ triboelectric nanogenerator for robust large-scale mechanical energy harvesting and instantaneous motion sensor applications. *Nano Energy*, 74: 104802. <https://doi.org/10.1016/j.nanoen.2020.104802>
- [12] Nguyen V, Yang R. (2013). Effect of humidity and pressure on the triboelectric nanogenerator. *Nano Energy*, 2(5): 604-608. <https://doi.org/10.1016/j.nanoen.2013.07.012>
- [13] Zhang JH, Hao X. (2020). Enhancing output performances and output retention rates of triboelectric nanogenerators via a design of composite inner-layers with coupling effect and self-assembled outer-layers with superhydrophobicity. *Nano Energy*, 76: 105074. <https://doi.org/10.1016/j.nanoen.2020.105074>
- [14] Ahn, J., Zhao, Z. J., Choi, J., Jeong, Y., Hwang, S., Ko, J., Gu, J., Jeon, S., Park, J., Kang, M., Del Orbe, D. V., Cho, I., Kang, H., Bok, M., Jeong, J. H., & Park, I. (2021). Morphology-controllable wrinkled hierarchical structure and its application to superhydrophobic triboelectric nanogenerator. *Nano Energy*, 85(March), 105978. <https://doi.org/10.1016/j.nanoen.2021.105978>
- [15] Shen J, Li Z, Yu J, Ding B. (2017). Humidity-resisting triboelectric nanogenerator for high performance biomechanical energy harvesting. *Nano Energy*, 40: 282-288. <https://doi.org/10.1016/j.nanoen.2017.08.035>
- [16] Lv, P., Shi, L., Fan, C., Gao, Y., Yang, A., Wang, X., Ding, S., & Rong, M. (2020). Hydrophobic Ionic Liquid Gel-Based Triboelectric Nanogenerator: Next Generation of Ultrastable, Flexible, and Transparent Power Sources for Sustainable Electronics. *ACS Applied Materials and Interfaces*, 12(13), 15012–15022. <https://doi.org/10.1021/acsami.9b19767>
- [17] Zhou, Q., Lee, K., Kim, K. N., Park, J. G., Pan, J., Bae, J., Baik, J. M., & Kim, T. (2019). High humidity- and contamination-resistant triboelectric nanogenerator with superhydrophobic interface. *Nano Energy*, 57(December 2018), 903–910. <https://doi.org/10.1016/j.nanoen.2018.12.091>
- [18] Ccorahua R, Cordero A, Luyo C, Quintana M, Vela E. (2019). Starch-Cellulose-Based triboelectric nanogenerator obtained by a low-cost cleanroom-free processing method. *MRS Adv*, 4(23): 1315-1320. <https://doi.org/10.1557/adv.2018.652>
- [19] Wang N, Zheng Y, Feng Y, Zhou F, Wang D. (2020). Biofilm material based triboelectric nanogenerator with high output performance in 95% humidity environment. *Nano Energy*, 77(May): 105088. <https://doi.org/10.1016/j.nanoen.2020.105088>

- [20] Wang J, Wu H, Fu S, Li G, Shan C, He W, Hu C. (2022). Enhancement of output charge density of TENG in high humidity by water molecules induced self-polarization effect on dielectric polymers. *Nano Energy*, 104(Part B): 107916. <https://doi.org/10.1016/j.nanoen.2022.107916>
- [21] Ccorahua R, Huaroto J, Luyo C, Quintana M, Vela EA. (2019). Enhanced-performance bio-triboelectric nanogenerator based on starch polymer electrolyte obtained by a cleanroom-free processing method. *Nano Energy*, 59(March): 610-618. <https://doi.org/10.1016/j.nanoen.2019.03.018>
- [22] Shi, L., Dong, S., Xu, H., Huang, S., Ye, Q., Liu, S., Wu, T., Chen, J., Zhang, S., Li, S., Wang, X., Jin, H., Kim, J. M., & Luo, J. (2019). Enhanced performance triboelectric nanogenerators based on solid polymer electrolytes with different concentrations of cations. *Nano Energy*, 64(August), 103960. <https://doi.org/10.1016/j.nanoen.2019.103960>
- [23] Zhu Z, Xia K, Xu Z, Lou H, Zhang H. (2018). Starch Paper-Based Triboelectric Nanogenerator for Human Perspiration Sensing. *Nanoscale Res. Lett*, 13: 4-9. <https://doi.org/10.1186/s11671-018-2786-9>
- [24] Torres FG, Troncoso OP, Torres C, Díaz DA, Amaya E. (2011). Biodegradability and mechanical properties of starch films from Andean crops. *Int. J. Biol. Macromol*, 48(4): 603-606. <https://doi.org/10.1016/j.ijbiomac.2011.01.026>
- [25] Ben Doudou B, Vivet A, Chen J, Laachachi A, Falher T, Poilâne C. (2014). Hybrid carbon nanotube - Silica/ polyvinyl alcohol nanocomposites films: Preparation and characterisation," *J. Polym. Res*, 21(4). <https://doi.org/10.1007/s10965-014-0420-9>
- [26] Kochkina NE, Butikova OA. (2019). Effect of fibrous TiO₂ filler on the structural, mechanical, barrier and optical characteristics of biodegradable maize starch/PVA composite films. *Int. J. Biol. Macromol*, 139: 431-439. <https://doi.org/10.1016/j.ijbiomac.2019.07.213>
- [27] Rajesh K, Crasta V, Rithin Kumar NB, Shetty G, Rekha PD. (2019). Structural, optical, mechanical and dielectric properties of titanium dioxide doped PVA/PVP nanocomposite. *J. Polym. Res*, 26(4): 4-10. <https://doi.org/10.1007/s10965-019-1762-0>
- [28] Sarkar S, Guibal E, Quignard F, SenGupta AK (2012). Polymer-supported metals and metal oxide nanoparticles: Synthesis, characterization, and applications. *J. Nanoparticle Res*, 14(2): 2-24. <https://doi.org/10.1007/s11051-011-0715-2>
- [29] Alvarez-Ramirez J, Vazquez-Arenas J, García-Hernández A, Vernon-Carter EJ. (2019). Improving the mechanical performance of green starch/glycerol/Li + conductive films through cross-linking with Ca²⁺. *Solid State Ionics*, 332(November): 1-9. <https://doi.org/10.1016/j.ssi.2019.01.002>
- [30] Abdullah AM, Aziz SB, Saeed SR(2021). Structural and electrical properties of polyvinyl alcohol (PVA):Methyl cellulose (MC) based solid polymer blend electrolytes inserted with sodium iodide (NaI) salt. *Arab. J. Chem*, 14(11): 103388. <https://doi.org/10.1016/j.arabjc.2021.103388>
- [31] Bergo P, Sobral PJA, Prizon JM. (2011). Effect of glycerol on physical properties of cassava starch films. *J. Food Process. Preserv*, 34(2): 401-410. <https://doi.org/10.1111/j.1745-4549.2008.00282.x>
- [32] Adamu AD, Jikan SS, Talip BHA, Badarulzaman NA, Yahaya S. (2017). Effect of glycerol on the properties of tapioca starch film. *Mater. Sci. Forum*, 888: 239-243. <https://doi.org/10.4028/www.scientific.net/MSF.888.239>
- [33] Abral H, Hartono A, Hafizulhaq F, Handayani D, Sugiarti E, Pradipta O. (2019). Characterization of PVA/cassava starch biocomposites fabricated with and without sonication using bacterial cellulose fiber loadings. *Carbohydr. Polym*, 206: 593-601. <https://doi.org/10.1016/j.carbpol.2018.11.054>
- [34] Surudžić, R., Janković, A., Bibić, N., Vukašinović-Sekulić, M., Perić-Grujić, A., Mišković-Stanković, V., Park, S. J., & Rhee, K. Y. (2016). Physico-chemical and mechanical properties and antibacterial activity of silver/poly(vinyl alcohol)/graphene nanocomposites obtained by electrochemical method. *Composites Part B: Engineering*, 85, 102–112. <https://doi.org/10.1016/j.compositesb.2015.09.029>

- [35] Wang Y, Zhang H, Zeng Y, Hossen Md A, Dai Y, Li S, Liu Y, Qin W. (2022). Development and characterization of potato starch/lactucin/nano-TiO₂ food packaging for sustained prevention of mealworms. *Food Packag. Shelf Life*, 33: 100-837. <https://doi.org/10.1016/J.FPSL.2022.100837>
- [36] Oleyaei SA, Almasi H, Ghanbarzadeh B, Moayedi AA. (2016). Synergistic reinforcing effect of TiO₂ and montmorillonite on potato starch nanocomposite films: Thermal, mechanical and barrier properties. *Carbohydrate Polymers*, 152: 263-262. <https://doi.org/10.1016/j.carbpol.2016.07.040>
- [37] Park, H. W., Huynh, N. D., Kim, W., Hwang, H. J., Hong, H., Choi, K. H., Song, A., Chung, K. B., & Choi, D. (2018). Effects of embedded TiO₂-x nanoparticles on triboelectric nanogenerator performance. *Micromachines*, 9(8). <https://doi.org/10.3390/mi9080407>
- [38] Bunriw, W., Harnchana, V., Chanthad, C., & Huynh, V. N. (2021). Natural rubber-TiO₂ nanocomposite film for triboelectric nanogenerator application. *Polymers*, 13(13), 1–12. <https://doi.org/10.3390/polym13132213>
- [39] Butyral, P., Anti, E., Agent, O., Benas, J., Huang, C., Yan, Z., Liang, F., & Li, P. (2022). Nanofiber-Based Odor-Free Medical Mask Fabrication Using Polyvinyl Butyral and Eucalyptus Anti Odor Agent. *Polymers* 2022, 14: 4447. <https://doi.org/10.3390/polym14204447>
- [40] Wang, N., Feng, Y., Zheng, Y., Zhang, L., Feng, M., Li, X., Zhou, F., & Wang, D. (2021). New Hydrogen Bonding Enhanced Polyvinyl Alcohol Based Self-Charged Medical Mask with Superior Charge Retention and Moisture Resistance Performances. *Advanced Functional Materials*, 31(14), 1–14. <https://doi.org/10.1002/adfm.202009172>
- [41] Patil, S., Bharimalla, A. K., Mahapatra, A., Dhakane-Lad, J., Arputharaj, A., Kumar, M., Raja, A. S. M., & Kambli, N. (2021). Effect of polymer blending on mechanical and barrier properties of starch-polyvinyl alcohol based biodegradable composite films. *Food Bioscience*, 44(PA), 101352. <https://doi.org/10.1016/j.fbio.2021.101352>